JOURNAL OF GEOPHYSICAL RESEARCH, VOL. 93, NO. C11, PAGES 14,099–14,105, NOVEMBER 15, 1988

Evaluation of Preliminary Experiments Assimilating Seasat Significant Wave Heights Into a Spectral Wave Model

DINORAH C. ESTEVA

Ocean Products Center, National Weather Service, National Oceanic and Atmospheric Administration, Washington, D. C.

Preliminary experiments dealing with the assimilation of significant wave heights (SWH) from the Seasat altimeter into the National Oceanic and Atmospheric Administration Ocean Wave (NOW) global spectral model are discussed. For all experiments, National Meteorological Center–analyzed winds for the Seasat period were used to drive the ocean surface. A hindcast was first made running the model with no assimilation for use as a control. The model was then run, using both simple replacement and a blending procedure to spread the influence of an observation to nearby grid points and for different assimilation frequencies. Forecasts of SWH from each assimilation run and the hindcasts are compared to the corresponding Seasat SWH estimate from subsequent satellite passes. Best results are obtained by using a 3-hour assimilation frequency with simple replacement and by scaling the forecasted spectrum with the observed SWH. A mean improvement of 7.7% (±8.4% at the 90% confidence level) is thus achieved for the 10 days of the experiment, with a maximum improvement of 25%.

INTRODUCTION

This paper presents the results of a preliminary investigation of techniques for incorporating wave measurements into wave-forecasting models and of their impact on model forecasts. Presently, the primary input to numerical wave models is a marine boundary layer wind field provided by an atmospheric model. The forecast skill of wave models is highly dependent on an accurate specification of this marine wind. While the assimilation of meteorological data into atmospheric models has become routine [*McPherson et al.*, 1979], the scarcity of wave data has precluded a parallel development in connection with wave models. The availability of satellite-borne sensors is rapidly changing this situation, making the assimilation of wave observations into wave models feasible.

Progress has been made on the theory of the growth and evolution of a wind sea spectrum [*Hasselmann*, 1968]; however, exact computation of the evolution process is still time consuming [*Hasselmann et al.*, 1985, *Hasselmann and Hasselmann*, 1985]. Although this computation technique may improve model forecasts, the inaccuracies in the wind fields used to drive the model will still remain. These inaccuracies can only be compensated for by the assimilation of good quality data.

While significant wave height (SWH) is the most readily available wave parameter, its inversion into a two-dimensional spectrum is not a unique process. Some assumptions about spectral shape, as well as means of differentiating between sea and swell, may be introduced to assist in this inversion. Other investigators are presently exploring the use of such procedures (J. P. Thomas, personal communication, 1987) and the wave-modeling group headed by Hasselmann advocates the introduction of a "wave age" in the assimilation problem. In the present study, only knowledge of SWH is assumed. Explicit assumptions about wind, sea, spectral shape, or the use of derived parameters to better define the wave field have been avoided. Evaluation of these preliminary experiments indicate that forecasts can be significantly improved by replacing the forecasted SWH with the observed SWH and scaling the forecasted spectrum accordingly.

Paper number 88JC03319.
0148-0227/88/88JC-03319$05.00

THE EXPERIMENTS

Analyzed winds, rather than wind forecasts, were used to drive the ocean surface for all runs. The winds were those for the corresponding Seasat period, resulting from the National Meteorological Center (NMC) Global Data Assimilation System. This analysis was based on Cressman's successive correction method [*McPherson et al.*, 1979], rather than the presently used optimum interpolation technique. A hindcast with no assimilation was first done to serve as a control (control run). For the assimilation runs, a 24-hour hindcast was done, assimilating SWH estimates from the Seasat altimeter into the National Oceanic and Atmospheric Administration Ocean Wave (NOW) global model [*Chin*, 1985] at constant time intervals. The resulting 24-hour wave field was used as the initial wave conditions for a 72-hour forecast. A brief description of NOW model characteristics is given later. Forecasts from the control run and each of the assimilation runs were compared to the corresponding altimeter estimates for subsequent satellite passes.

The assimilation of SWH into the directional spectrum was done by scaling the forecasted spectral components with the ratio $(H_o/H_f)^2$, where H_o and H_f are the observed and forecasted SWH, respectively. Thus the total energy under the modified spectrum will correspond to the observed SWH, while the shape of the distribution of energy in frequency and direction remains unchanged. This approach assumes that the model correctly predicts the proportion of energy in the "sea" and swell portions of the spectrum. Its success depends on how well the transition from sea to swell is modeled and on the stage of wave development. In one of the experiments, no blending was done. That is, the influence of an observed SWH was confined to the one grid point at which the observation existed. In the other experiment the influence of the observation was spread to the surrounding grid points by preserving the local slopes in the forecasted SWH field. No distinction between sea and swell was made in the blending.

The blending procedure proved to be highly sensitive to model forecast errors. When the model incorrectly forecasts the geographical location of high and low waves, the blending

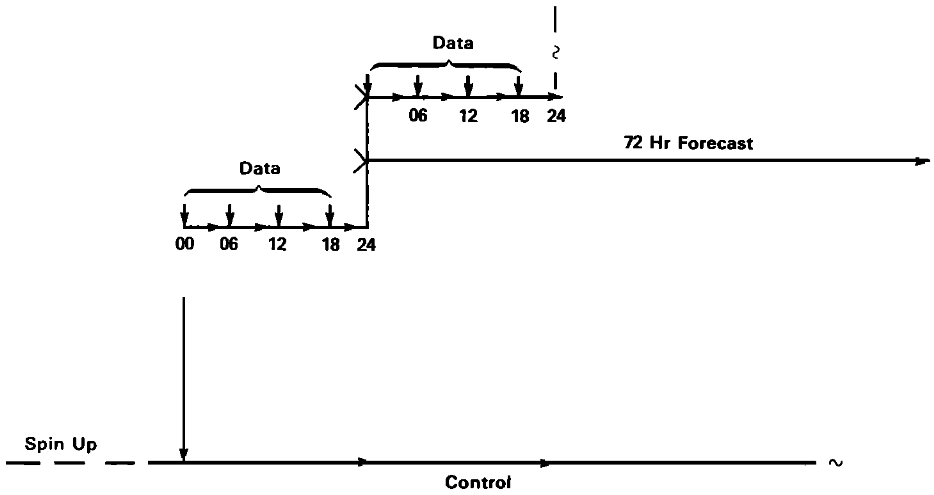

Fig. 1. Six-hour assimilation cycle. Vertical arrows indicate data insertion; horizontal arrows indicate forecast.

contributes to further increase SWH at the predicted areas of high waves and to decrease those at areas of low waves, thus increasing forecast error. Use of the blending caused 47% of the forecasts to be degraded; for this reason, the technique was abandoned in favor of simple replacement. In addition, except for the longer swells, waves are a localized phenomenon, so simple replacement is preferable to blending when no distinction between sea and swell is introduced. Only results using simple replacement at 6-hour intervals will be presented in detail. Figure 1 illustrates the scheme.

SEASAT DATA SET AND DATA REDUCTION

Besides providing a measure of range (distance), radar altimeters may provide estimates of SWH and wind speed [*McMillan*, 1981]. The Seasat altimeter provided 1-s averages of these values over a footprint varying in area from 2 to 7 km [*Queffeulou*, 1983]. The assimilation experiments used 13 days of the Seasat altimeter SWH from September 16–28, 1978. Along-track sections of 17-s duration, with a one point overlap from section to section, were edited separately to eliminate outliers and questionable values. For each section, individual values departing four standard deviations or more from the mean were replaced with linearly interpolated values. Groups of two or more consecutive values failing this test were discarded.

The edited SWH for each 3-hour interval centered at the model forecast times and within each 2.5° by 2.5° square around the model grid points were averaged and assigned to the grid point and hour. Further screening was done by discarding those averages with a standard deviation larger than or equal to one half of its value and averages of fewer than three values. These gridded values were used both in the assimilation and for comparisons with the model forecasts.

The bias, mean absolute error (MAE), and root-mean-square (rms) error, as given by (1), were used for evaluating results.

$$\begin{aligned} \text{bias} &= N^{-1}\Sigma(H_{fn} - H_{on}) \\ \text{MAE} &= N^{-1}\Sigma|H_{fn} - H_{on}| \\ \text{rms} &= [N^{-1}\Sigma(H_{fn} - H_{on})^2]^{1/2} \end{aligned} \tag{1}$$

where $n = 1 \cdots N$, the total number of observations, H_{on} and H_{fn} are the nth observed and forecasted SWH at a grid point, respectively.

THE NOW MODEL

The global model used in this study may be termed a discrete/hybrid model in the terminology of Sea Wave Modeling Project (SWAMP) [*The SWAMP Group*, 1985] because it combines aspects of both the Pierson-Tick-Baer-type models [*Pierson et al.*, 1966] and parametric models. Wave growth is modeled by a nonlinear parametric algorithm based on Hasselmann's fetch law, as developed in the Sea Air Interaction Laboratory (SAIL) II coding described by *Greenwood et al.* [1985], combined with a wind-wave instability mechanism compatible with the *Snyder et al.* [1981] results. The spectral growth is limited by a modified JONSWAP upper limit, whereby the peak enhancement parameter does not exceed 2.9. Directional band relaxation and Mitsuyasu's spreading function, modified to be zero in the upwind quadrants, are used.

The model spectrum has 24 directional bands spaced at 15° intervals, with the first band centered at 7.5°, and 15 frequency bands from 0.03889 to 0.30833 Hz. It forecasts waves from 70°S to 75°N every 3 hours on a 2.5° by 2.5° latitude and longitude grid.

A downstream interpolation propagation scheme [*Greenwood et al.*, 1985] is performed over the 2.5° by 2.5° grid in two 1.5-hour steps per model 3-hour step.

Fields used by the model are the 1000-mbar components of the wind speed, sea surface water temperature, the 1000-mbar air temperature, and the surface pressure distribution. These are used to compute the wind direction and speed at 19.5 m above the sea surface and the friction velocity using Cardone's marine boundary layer model [*Cardone*, 1969].

THE ASSIMILATION EXPERIMENT

September 16, 1978, was chosen as the start of the assimilation experiment, because there were a relatively large number of observations available. The model was started from a flat sea on September 11, so that by September 16 a fair resemblance of real wave conditions existed over all oceans. The control run was continued through September 28. Assimilation and simple replacement were done every 6 hours on September 16 and the resulting 24-hour field was used to initialize a 72-hour forecast on September 17 (Figure 1). The procedure was repeated on all subsequent days through September 26. Only observations differing by 0.5 m or more from

TABLE 1. Total Number of Observations Assimilated Per Day at the Different Latitudes

Day	Latitude 65°–30°S	Latitude 30°S–0°	Latitude 0°–30°N	Latitude 30°–65°N	Total
Sept. 16	249	110	82	78	519
Sept. 17	222	106	65	110	503
Sept. 18	198	92	64	79	433
Sept. 19	216	82	57	66	421
Sept. 20	185	86	61	109	441
Sept. 21	187	73	38	78	376
Sept. 22	228	98	66	60	452
Sept. 23	247	94	76	71	488
Sept. 24	236	81	78	79	474
Sept. 25	226	108	94	59	487
Totals	2194	930	681	789	4594

the forecasted value were assimilated. Table 1 gives the daily total number of observations assimilated at the different latitudes. It can be seen from Table 1 that for a given hour the number of observations assimilated can be small. The situation would improve if more than one satellite were available.

Results

Since the Seasat altimeter SWH have been ground-proofed [*Fedor and Brown*, 1982], forecasts from the control run provide an excellent opportunity for evaluating the performance of the NOW model globally. In addition, insight is gained about the results of the assimilation from a detailed comparison of the control run hindcast and the Seasat SWH for the corresponding passes.

Results From the Control Run

An idea of the magnitude of the errors involved is given by Figures 2 and 3. The rms error and MAE computed for all hindcasts for the 10 days (September 17–26) of the control run are grouped as follows: observed SWH higher than 0.5, 2, 4, and 6 m, and for what would be the forecast for day 1, 2, and 3 in a 72-hour forecast. At each SWH category in Figures 2 and 3 the errors corresponding to hindcasts for days 1, 2, and 3 are plotted. It is evident that errors increase for the higher waves. This increase is probably due to a combination of two factors: (1) the wave model underforecasted the higher waves (H. Chin, private communication, 1987), and (2) deterioration

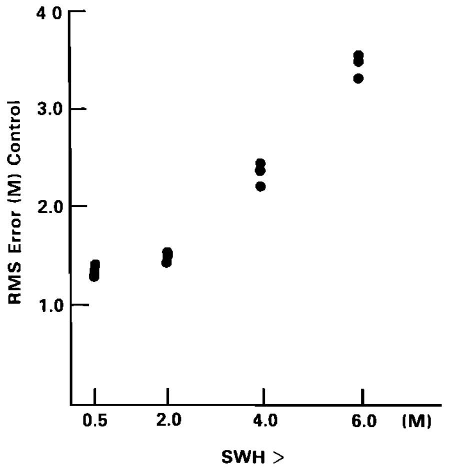

Fig. 2. The rms errors (in meters) for SWH grouped according to height for the control run: observed SWH higher than 0.5, 2, 4, and 6 m.

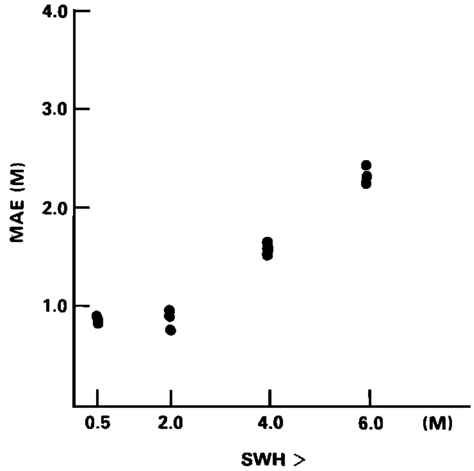

Fig. 3. MAE (in meters) for SWH grouped according to height for the control run: observed SWH higher than 0.5, 2, 4, and 6 m.

of the altimeter estimates for higher waves [*Fedor and Brown*, 1982].

Values of the bias, MAE, and rms for all hindcasts for SWH higher than 0.5 m and for the same 10 days of the control run, are stratified by latitude in Table 2. Errors are largest in the southernmost latitudes because of the sparsity of wind observations; hence the wind analyses have larger errors. SWH are usually lower in the equatorial regions, thus errors are smaller here. A possible reason for the large errors at the northern latitudes is discussed later.

Results From the Assimilation Run

It should be noted that the full impact of the assimilation cannot be fully assessed because of the lack of information in areas outside of the satellite ground track. During a 3-hour interval the satellite ground track may be in regions where the impact of the assimilation is favorable, while during other 3-hour periods, the reverse may be true. As will be seen, the results indicate that the overall impact of the assimilation is favorable.

The distributions of absolute error for all hindcasts for the control (dashed curve) and forecasts for the assimilation (solid curve) runs are shown in Figures 4(*a*) through 4(*d*) for different SWH categories. All of the distributions show that the assimilation has improved the forecasts.

Table 3 shows the ratios of the bias, MAE, and rms for the assimilation to the control runs for all forecast hours, stratified by latitude. Greatest improvements are in the southern equatorial belt, where waves usually are not high and the winds are sparse.

Table 4 gives the daily correlation coefficients between the altimeter SWH and the forecasts for the control and assimi-

TABLE 2. Bias, MAE, and rms for September 17 Through September 26 for SWH Greater Than 0.5 m for Different Latitudes

Latitude Range	Bias, m	MAE, m	rms, m
30.0°–62.5°N	−0.50 ± 2.2	0.83 ± 1.8	1.40
0°–30.0°N	0.12 ± 1.6	0.55 ± 1.3	0.97
30.0°S–0	−0.11 ± 1.3	0.58 ± 0.85	0.78
62.5°–30.0°S	0.37 ± 2.9	1.28 ± 2.05	1.79

All hindcasts (September 17–26) are from the control run. Plus or minus signs indicate confidence limits.

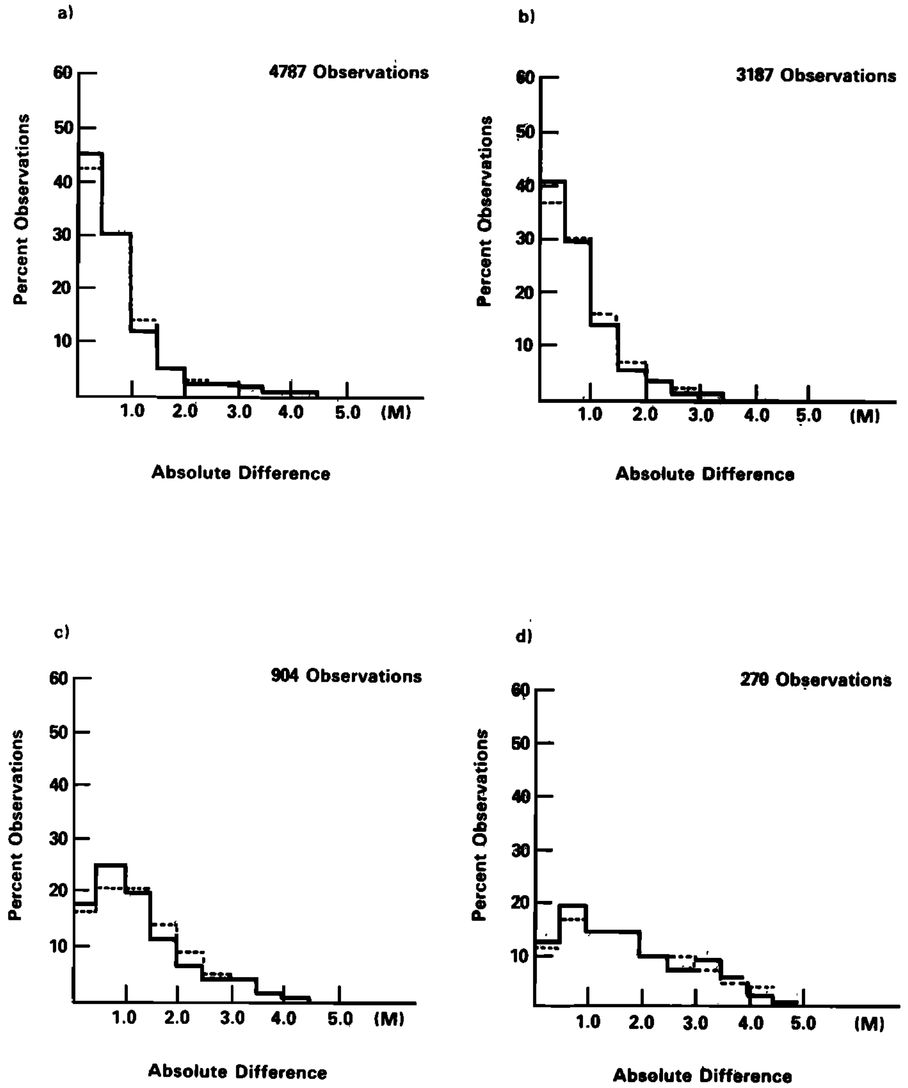

Fig. 4. Distribution of MAE for the control run (dashed curve) and for the assimilation run (solid curve), all forecasts, (*a*) for SWH higher than 0.5 m; (*b*) for SWH higher than 2 m; (*c*) for SWH higher than 4 m; (*d*) for SWH higher than 6 m.

lation runs. The correlations are not high, and the improvements in correlation due to the assimilation are slight. This implies that the analyzed winds, and thus the forecast waves, are not depicting the geographical distribution of highs and lows accurately.

The daily impact of the assimilation may be seen from the ratios of MAE of the assimilation to the control run forecasts for each day at the different latitudes. Figures 5, 6, and 7 show these ratios for SWH higher than 0.5, 2 and 4 m, respectively. There were no SWH higher than 4 m in the northern equatorial belt. Largest improvements are for waves higher than 2 m, with improvements of the order of 20% achieved on some days. Considering the magnitude of the errors obtained for the control run, the achieved improvements bring the errors close to the altimeter specification of 0.5 m.

The variation in forecast improvement with assimilation may be explained partially by variations in the correlation of the analyzed winds with the altimeter winds, as discussed in

TABLE 3. Ratios of Bias, MAE, and rms Error for the Assimilation to Control Runs for September 17 Through September 26 for SWH Greater Than 0.5 m for Different Latitudes

Latitude Range	Bias, m	MAE, m	rms, m
30.0°–62.5°N	0.91	0.99	0.98
0°–30.0°S	1.30	0.98	0.99
30.0°S–0°	0.36	0.91	0.94
62.6°–30.0°S	1.03	0.96	0.97

TABLE 4. Daily Correlations Between Altimeter and Forecast SWH

Day	Control	Assimilation
Sept. 17	0.63	0.66
Sept. 18	0.61	0.62
Sept. 19	0.54	0.56
Sept. 20	0.58	0.59
Sept. 21	0.61	0.62
Sept. 22	0.61	0.62
Sept. 23	0.61	0.62
Sept. 24	0.53	0.54
Sept. 25	0.55	0.56
Sept. 26	0.58	0.59

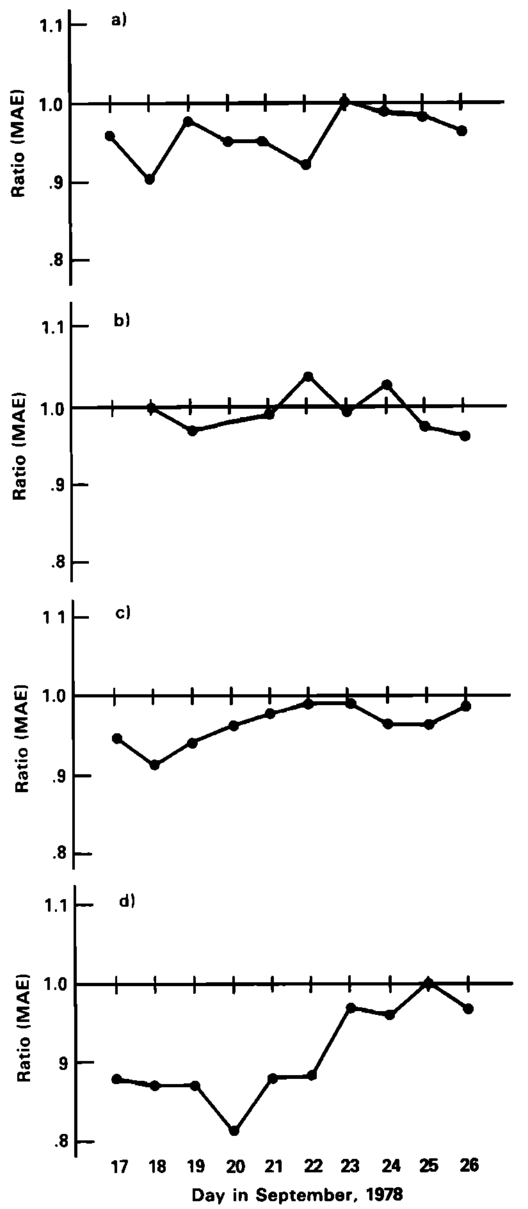

Fig. 5. Ratios of MAE for assimilation to control runs, for each day of the experiment, for SWH higher than 0.5 m. Latitudes are (*a*) between 0.0° and 30.0°N; (*b*) 30.0° and 62.5°N; (*c*) 62.5° and 30.0°S; and (*d*) 30.0°S and 0.0°

the next paragraph. Daily correlations between the midnight (0000 UT) analyzed winds and the altimeter wind speed (edited and gridded in the same way as the SWH) are given in Figure 8.

Although the wind correlations are for only one analysis hour (0000 UT) and the improvements in wave forecasts plotted in Figure 5 are for the whole day, it can be seen that the improvements have a tendency to increase with a decrease in wind correlation. It is surprising that wind correlations are similar and low in both hemispheres. Several factors may contribute to the low correlations; one is that the 1000-mbar data produced by the analysis may not necessarily be at the ocean surface, while the altimeter estimates are for the surface wind; another is the difference in the scale of the two data sets. Yet another factor is the different time windows for the two data sets. The in situ observations which go into the analysis are synoptic observations, usually taken within 20 min of the synoptic hour, while in this study a 1.5-hour window on either side of the synoptic hours was imposed on the altimeter estimates. *Fedor and Brown* [1982] find a correlation of 0.86 between the Seasat altimeter winds and NOAA Data Buoy Center (NDBC) buoy winds (for wind speeds under 10 m/s) and an rms error of 1.58 m/s. They used a 1.5-hour window and an 80-km distance approach between the buoy location and the satellite ground track. Only 87 observations during September and October satisfied these restrictions and were used in their comparison. It is thus concluded that the variation in forecast improvement achieved with the assimilation is partially explained by the variation in correlation of the NMC-analyzed winds with the observed winds, since it is to be expected that there is less room for improvement in the SWH when winds are better correlated. For 2 days, September 19 and September 25, the wind correlation in the northern hemisphere is small and negative. This may explain the unexpectedly large errors in the northern latitudes found for the control run (Table 2).

Two Additional Experiments

In order to establish whether a less frequent assimilation is acceptable or whether a more frequent assimilation results in significant improvements, two additional experiments were

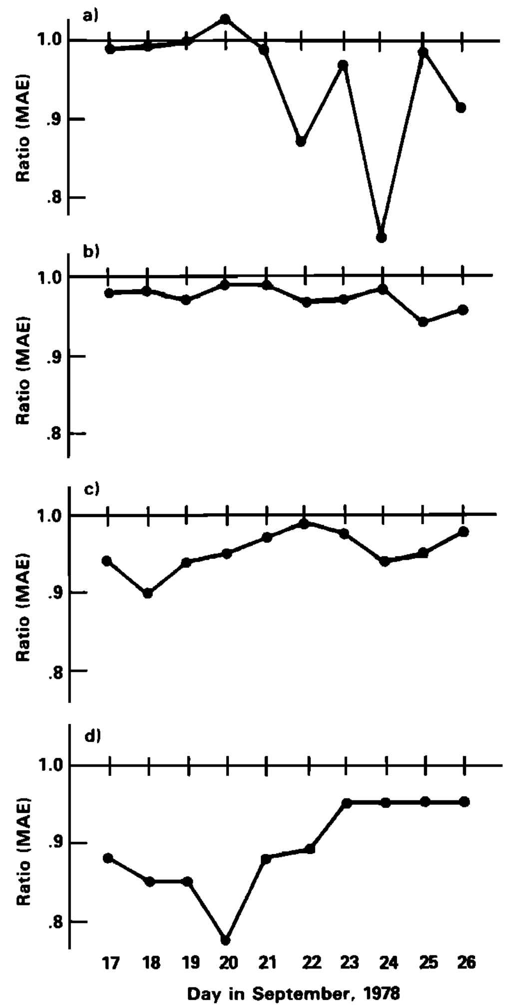

Fig. 6. Same as Figure 5, except for SWH higher than 2 m.

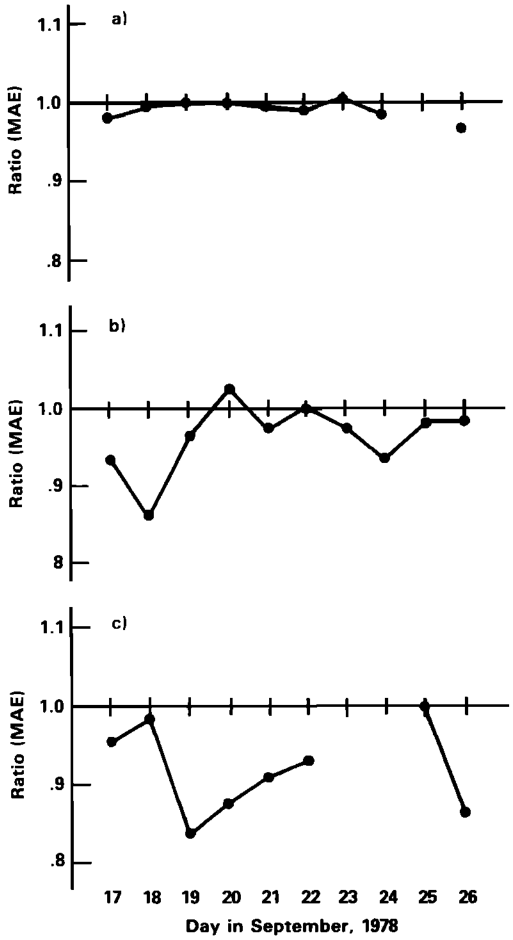

Fig. 7. Ratios of MAE for assimilation to control runs for SWH higher than 4 m. Latitudes are (*a*) between 30.0° and 62.5°N; (*b*) 62.5° and 30.0°S; and (*c*) 30.0°S and 0.0°. There were no SWH higher than 4 m for the northern equatorial belt.

performed. For one the assimilation was done at 12-hour intervals, while for the other a 3-hour interval was used.

Table 5 shows the percentages of forecasts improved, degraded, and left unchanged for these two experiments, along with those for the 6-hour assimilation interval. The mean percent improvement in MAE for the 6-hour assimilation frequency was 3.8%, with a 90% confidence limit of 6.2% (day 1 forecasts). For the 3-hour assimilation frequency, the mean percent improvement and 90% confidence limits were 7.76% and 8.4%, respectively. On the basis of these results, a 3-hour assimilation frequency appears desirable.

Note that the percentage of forecasts improved by the assimilation increases with the frequency of the assimilation. This is due to the fact that at each synoptic hour the satellite ground track is at a different location on the globe. As the frequency of the assimilation increases, these portions of the globe are closer together and, although each section is assimilated at a different time, the local improvements introduced by each assimilation step are propagated during the next model step to other areas of the globe. Degradation of the forecasts may result when poor observations, which escaped the limited editing done to the data are assimilated, or when the forecasted spectrum is in error, either with regard to the total energy, or to the partition between sea and swell. For example, the assimilation may increase the energy at frequencies where the model has overpredicted, or it may decrease it further at frequencies at which the model is underpredicting.

CONCLUSIONS

Assimilation of SWH alone does improve forecasts. The improvement is inversely related to the correlation between altimeter winds and the analyzed winds used to drive the ocean wave model.

The improvements in SWH forecasts achieved in this study are small. It is believed the small improvement is due to two factors: (1) the inadequate global coverage afforded by one polar-orbiting satellite, and (2) the use of analyzed winds rather than forecast winds. Analyzed winds are not available when producing wave forecasts in an operational mode. In such a mode, forecast winds would be used to drive the ocean surface. Since forecast winds have larger errors than analyzed winds, a greater impact of the assimilation may be expected in an operational mode.

Since waves are a relatively localized phenomenon, the technique of simple replacement of the forecasted SWH with the observed SWH works better than a blending technique when no distinction between sea and swell is made. In such a case the blending introduces erroneous energy in the swell and sea portions of the spectrum and leads to degradation of the forecasts. Distinction between sea and swell cannot be made without introducing additional information or assumptions into the assimilation and blending schemes.

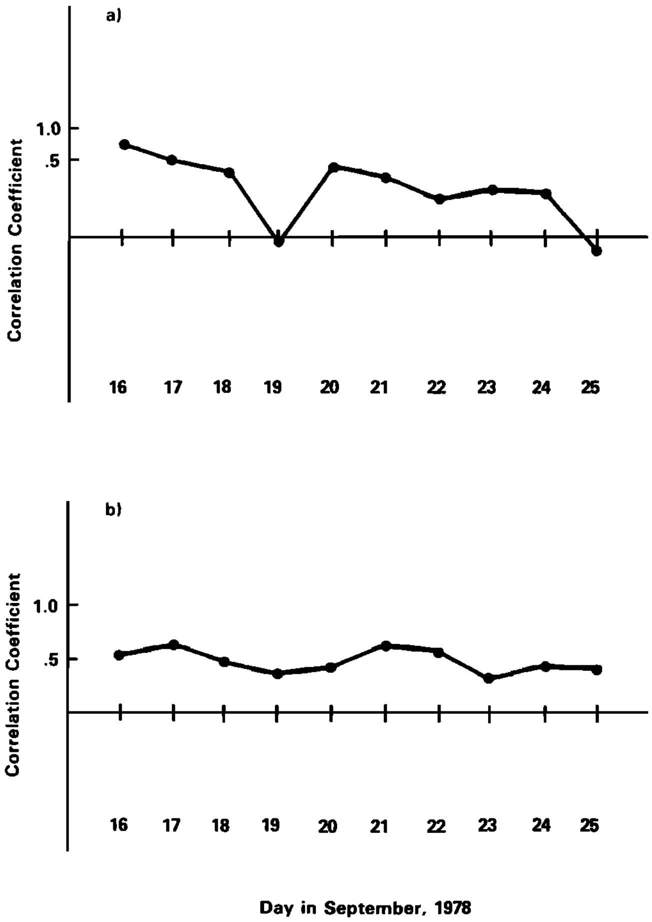

Fig. 8. Correlation coefficient between altimeter winds and NMC analysis for midnight (0000 UT) each day. (*a*) Northern hemisphere; (*b*) southern hemisphere.

TABLE 5. Comparison of Results With Different Assimilation Frequency

	Frequency, hours		
	12	6	3
Percent improved	66	72	82
Percent degraded	25	20	16
Percent unchanged	9	8	2
Maximum improvement, %	12	16	25

Correlations between altimeter SWH and wind speeds with forecasted SWH and analyzed winds, respectively, are small, indicating poor skill in the location of areas of highs and lows. This situation might be improved by developing the capability of blending the altimeter winds into the surface wind analyses. This will result in a more accurate distribution of the areas of high and low winds in the resulting analyzed fields, thus improving forecasts of areas of high and low waves and further improving the effects of a blending technique for SWH.

Acknowledgments. The author appreciates the helpful discussions and suggestions provided by D. B. Rao and H. Chin during the course of this study. This paper is Ocean Products Center Contribution 19.

REFERENCES

Cardone, V. J., Specification of the wind distribution in the marine boundary layer for wave forecasting, *Geophys. Sci. Lab. Tech. Rep. TR69-1*, N. Y. Univ. Sch. of Eng. and Sci., New York, Dec. 1969.

Chin, H., An operational global-scale spectral ocean wave forecasting model, in *Ocean 85 Conference Record*, vol. 2, pp. 110–111, Marine Technology Society, IEEE Council of Ocean Engineers, San Diego, Calif., 1985

Fedor, L. S., and G. S. Brown, Waveheight and wind speed measurements from the Seasat radar altimeter, *J. Geophys. Res.*, *87*, 3254–3260, 1982.

Greenwood, J. A., V. J Cardone, and L. M. Lawson, Intercomparison test version of the sail wave model, in *Ocean Wave Modeling*, pp. 221–233, Plenum, New York, 1985.

Hasselmann, K., Weak interaction theory of ocean waves, in *Basic Developments in Fluid Dynamics*, vol. 2, edited by M. Holt, pp. 117–182, Academic, San Diego, Calif., 1968.

Hasselmann, S., and K. Hasselmann, Computations and parameterizations of the nonlinear energy transfer in a gravity-wave spectrum, I, A new method for efficient computations of the exact nonlinear transfer integral, *J. of Phys. Oceanogr.*, *15*, 1369–1377, 1985.

Hasselmann, S., and K. Hasselmann, J. H. Allender, T. P. Barnett, Computations and parameterizations of the nonlinear energy transfer in a gravity-wave spectrum, II, Parameterizations of the nonlinear energy transfer for application in wave models, *J. of Phys. Oceanogr.*, *15*, 1378–1391, 1985.

McMillan, J. D., A global atlas of GEOS-3 significant wave height data and comparison of the data with national buoy data, *NASA Contract. Rep.*, *NASA-CR-156882*, Nov. 1981.

McPherson, R. D., K. H. Bergman, R. E. Kistler, G. E. Rasch, and D. S. Gordon, The NMC Operational Global Data Assimilation System, *Mon. Weather Rev.*, *107*, 1445–1461, 1979.

Pierson, W. J., L. J. Tick, and L. Baer, Computer-based procedures for preparing global wave forecasts and wind field analyses capable of using wave data obtained by a spacecraft, in *Proceedings of the 6th Naval Hydrodynamics Symposium*, pp. 499–532, U.S. Navy, Washington, D. C., 1966.

Queffeulou, P., Seasat Wave Height Measurement: A comparison with sea-truth data and a wave forecasting model—Application to the geographic distribution of strong sea states in storms, *J. Geophys. Res.*, *88*, 1779–1788, 1983.

Snyder, R. L., F. W. Dobson, J. A. Elliot, and R. B. Long, Array measurements of atmospheric pressure fluctuations above surface gravity waves, *J. Fluid Mech.*, *102*, 1–59, 1981.

The SWAMP Group, *Ocean Wave Modeling*, 256 pp., Plenum, New York, 1985.

D. C. Esteva, National Meteorological Center, National Weather Service, NOAA, WWB, W/NMC21, Room 206, Washington, DC 20233.

(Received March 21, 1988;
accepted May 31, 1988.)